# Novel Macromolecular Epoxy Resin Curing Agent Containing Biphenyl and Maleimide Moieties: Preparation, Curing Kinetics, and Thermal Properties of Its Cured Polymer

**Fei Guo, Xin-Nian Xia, Yuan-Qin Xiong, Jia Liu, Wei-Jian Xu**

*College of Chemistry and Chemical Engineering, Hunan University, Changsha 410082, People's Republic of China*

Received 27 January 2011; accepted 7 May 2011
DOI 10.1002/app.34851
Published online 16 December 2011 in Wiley Online Library (wileyonlinelibrary.com).

**ABSTRACT:** A new curing agent containing maleimide and biphenyl moieties (MIBP) was synthesized by the condensation polymerization of 4,4′-bismethoxymethylbiphenyl and *N*-(4-hydroxyphenyl)maleimide (HPM). The chemical structure was characterized with Fourier transform infrared (FTIR) spectroscopy, and the molecular weight of the new curing agent was determined by gel permeation chromatography. Curing reactions of *O*-cresol formaldehyde epoxy (CNE) resin with MIBP were investigated under nonisothermal differential scanning calorimetry, and the exotherm exhibited two overlapping exothermic peaks during the curing process; this was demonstrated by FTIR traces. The Flynn–Wall–Ozawa and Friedman methods were used to examine the kinetic parameters and the kinetic models of the curing processes of the CNE/MIBP mixtures. Both reactions turned out to be *n*th-order curing mechanisms. Values of the reaction order ($n$) = 1.42 and activation energy ($E_a$) = 91.2 kJ/mol were obtained for the first reaction of the curing of the CNE/MIBP system, and values of $n$ = 1.11 and $E_a$ = 78.7 kJ/mol were obtained for the second reaction. The thermal properties of the cured resin were measured with thermogravimetric analysis, and the results show a high glass-transition temperature ($T_g$ = 155°C), good thermal stability (temperature at 10% weight loss, under nitrogen and in air, ≈ 400 and 408°C, respectively), and high char yield (temperature = 800°C, char residue = 44.5% under nitrogen). These excellent thermal properties were due to the introduction of the maleimide and biphenyl groups of MIBP into the polymer structure. © 2011 Wiley Periodicals, Inc. J Appl Polym Sci 125: 104–113, 2012

**Key words:** epoxy resin curing agent; cure kinetics; maleimide; biphenyl; thermal properties

## INTRODUCTION

Up to now, research efforts on improving the properties of epoxy resins are still attractive for advanced applications. For example, cured epoxy resins with superior thermal stability are expected to be used as molding compounds and encapsulation materials in advanced electronic components.[1,2]

The ultimate properties of cured epoxy resins depend mainly on the structures of the epoxy resins and the curing agents. For these reason, modifications of epoxy resins or curing agents in both the backbone and pendant groups have been continuously investigated to improve the thermal and physical properties of cured epoxy resins. Many studies have been reported that improved the heat resistance of epoxy resins by increasing the crosslink density of the cured epoxy resin[3] or by introducing bulky structures, such as dicyclopentadiene,[4] biphenyl,[5,6] naphthalene,[7,8] fluorine, or maleimide.[9–11]

On the other hand, imide polymers are known for their high thermal stability, and it has been well reported in the literature that when chemical structures of the cured epoxy polymers are constituted with aromatic and/or heterocyclic rings, their thermal resistance is superior to those based on flexible or aliphatic chains.[12] Therefore, the use of imide groups to modify the structure of epoxy to enhance its thermal resistance has received great attention in the research community. However, in the introduction of imide groups into the backbone structure of epoxy resin, a difficulty in the processing ability was encountered.[13] Another way to improve the thermal resistance of epoxy is to use a curing agent containing imide groups, such as hydroxyl-terminated imide compounds, imide acid,[14] imide amine,[15,16] maleimide,[17] or imide anhydride.[18,19]

In this study, a novel curing agent containing maleimide and biphenyl moieties (MIBP) was synthesized. The resulting compound was used as a curing agent for CNE. Both the hydroxyl and maleimide groups in MIBP involved the curing reactions to form a highly crosslinking network. The curing kinetics of the CNE and MIBP blend (CNE/MIBP

*Correspondence to:* W.-J. Xu (weijianxu59@gmail.com).
Contract grant sponsor: Natural Science Foundation of Hunan; contract grant number: 2008FJ3116.
Contract grant sponsor: BaLing Petrochemical of China.

mixture) were investigated with a nonisothermal differential scanning calorimetry (DSC) technique. The kinetic parameters and the kinetic models of the curing processes of the CNE/MIBP mixtures were determined with the Flynn–Wall–Ozawa and Friedman methods. The thermal properties of the cured CNE resin with MIBP (CNE/MIBP polymer) were evaluated with thermogravimetric analysis (TGA) and compared with commercial curing agents [phenol formaldehyde novolac (PN), 4,4′-diaminodiphenylmethane (DDM), and 4,4′-diaminodiphenylsulfone (DDS)].

## EXPERIMENTAL

### Materials

DDS (97%), DDM (97%), *p*-aminophenol (99%), maleic anhydride (98%), and *p*-toluenesulfonic acid (*p*-TSA; 99%) were purchased from Shanghai Chemicals (Shanghai, China). 4,4′-Bismethoxymethylbiphenyl (BMB) were commercially obtained and were used without further purification. PN, used as curing agent with a hydroxyl equivalent weight of about 126 g/equiv, and CNE (CTDCN-200, epoxy equivalent weight = 207 g/equiv) were kindly supplied by BaLing Petrochemical of China. Triphenylphosphine was used as a curing accelerator. All of the solvents were reagent grade and were used without further purification.

### Synthesis of HPM

HPM was synthesized by a two-step reaction procedure from *p*-aminophenol and maleic 4anhydride, as previously described.[20] The chemical structure was characterized by Fourier transform infrared (FTIR) spectroscopy and elemental analysis (EA).

FTIR (KBr, $cm^{-1}$): 3481 (Ph—OH), 1705 (C=O symmetrical stretching), 1369 (C—N stretching), 714 (C=O bending), 688 (C=C bending). ANAL. Found: C, 63.51%; H, 3.68%; N, 7.44%. Calcd: C, 63.49%; H, 3.70%; N, 7.41%.

### Synthesis of MIBP

Into a 100-mL, three-necked round-bottom flask equipped with a Dean–Stark trap was added BMB (4.0 g, 1.65 mmol), HPM (6.7 g, 3.54 mmol), and *p*-TSA (0.05 g, 0.03 mmol). The mixture was heated at 115°C with magnetic stirring under a nitrogen atmosphere, and the reaction was continued for 5 h. The methanol generated from the polycondensation process was removed simultaneously by distillation. After cooling down to room temperature, the reaction mixture was washed with deionized water to give a neutralized solution and was then washed with ethanol five times to remove the unreacted raw materials. Subsequently, the product was dried at 60°C *in vacuo* for 8 h. As a result, a light yellow solid powder was obtained (8.7 g). The chemical structure was characterized by FTIR spectroscopy. The molecular weight was determined by gel permeation chromatography (GPC), which also confirmed the absence of unreacted monomers in the polymer. The hydroxyl equivalent weight was 328 g/equiv.

### Preparation of the cured epoxy resins

The cured epoxy resins were obtained from thermal curing of CNE with MIBP. For comparison purposes, commercially available PN and the commonly used aromatic amine curing agents DDM and DDS were also used as curing agents. Certain amounts of CNE and curing agents were mixed together according to molar stoichiometric ratios of phenolic hydroxyl or amino to epoxy of 1 : 1 with triphenylphosphine (2 wt % of the CNE) as a curing accelerator. The mixture was dissolved in methyl isobuthyl ketone to form a solution. The solvent was removed by vacuum stripping at 70°C for 12 h, and then, we cured the sample in an oven. The conditions of the curing reaction for the MIBP/CNE blend were determined from DSC, which were 130°C for 1 h, 180°C for 2 h, and 220°C for 2 h. The epoxy resins cured with PN (CNE/PN), DDM (CNE/DDM), and DDS (CNE/DDS) used as a control were prepared according to the literature.[16,21]

### Measurements

FTIR spectroscopy was recorded with a WQF-410 spectrophotometer (Beijing Rayleigh Analytical Instrument Co., Ltd., Beijing, China) with KBr pellets. EA was carried out on a Heraeus CHN-O Rapid Analyzer. GPC analysis was performed with a Waters 1525/2414 GPC instrument (Waters Corp. Ashland, Massachusetts). Waters Styragel column sets were used with a 1.0 mL/min flow rate of tetrahydrofuran and were calibrated by polystyrene standards.

The cure kinetic analysis was conducted by an STA 409 differential scanning calorimeter (Netzsch, Bavaria, Germany) with heating rates (β's) of 2.5, 5, 10, 15, and 20°C/min ranging from 50 to 300°C. Nitrogen gas was purged at a flow rate of about 50 mL/min. Calibration of the calorimeter was conducted for each β on the indium standard. With the presumption that the heat flow ($dQ/dt$) as measured by DSC was proportional to the rate of reaction ($d\alpha/dt$, also known as the cure rate), it was possible to determine the extent of fractional conversion ($\alpha$, also known as the degree of cure) directly from the experimental curve by partial integration.

TGA was determined with an STA-449C (Netzsch) at a β of 10°C/min under a nitrogen or air atmosphere, and the temperature ranged from room temperature to 800°C.

X-ray diffraction (XRD) spectroscopy was performed with Bruker D8-Advance X-ray diffraction equipment (Germany) under the following conditions: Cu target Kα ray [wavelength of the X-ray radiated from CuKα (λ) = 1.54187 Å], scanning voltage = 40 kV, scanning current = 40 mA, scanning speed = 0.5°/s, and scanning step = 0.02°.

## KINETIC ANALYSIS

The cure kinetics of a thermosetting polymer is conveniently monitored by DSC. $dQ/dt$ measured in DSC is proportional to both the overall heat release and $d\alpha/dt$:[22]

$$\frac{dQ}{dt} = Q_{\text{cure}}\frac{d\alpha}{dt} = Q_{\text{cure}}k(T)f(\alpha) \tag{1}$$

where $t$ is the time, $Q_{\text{cure}}$ is the total heat released when an uncured sample is brought to complete cure, α is the extent of a monomer conversion to a crosslinked network, $k(T)$ is the Arrhenius rate constant, and $f(\alpha)$ is the differential conversion function depending on the reaction mechanism. The rate constant ($k$) is dependent on temperature according to the Arrhenius equation shown in eq. (2):

$$k(T) = A\exp\left(-\frac{E_a}{RT}\right) \tag{2}$$

where $A$ is the pre-exponential factor and $E_a$ is the activation energy, which are Arrhenius parameters, and $R$ is the gas constant (8.314 J mol$^{-1}$ K$^{-1}$).

The explicit temperature dependence of $k$ is introduced by the replacement of $k(T)$ with the Arrhenius equation, which gives

$$\frac{d\alpha}{dt} = A\exp\left(-\frac{E_a}{RT}\right)f(\alpha) \tag{3}$$

Kinetic analysis of a nonisothermal resin-cured system in which a sample is heated at a constant rate is eliminated through the trivial transformation

$$\frac{d\alpha}{dT} = \frac{A}{\beta}\exp\left(-\frac{E_a}{RT}\right)f(\alpha) \tag{4}$$

where $\beta = dT/dt$ is a constant heating rate.

Kinetic analysis of a nonisothermal resin-cured system can be performed by the multiple β's. Two different isoconversional methods employed in this study were as follows, and the advantage of the two kinetics methods is that they do not require prior knowledge of the reaction mechanism to quantify kinetic parameters.[23]

### Flynn–Wall–Ozawa method

The isoconversional integral method was also proposed independently by Flynn, Wall, and Ozawa[24,25] with Doyle's approximation of the temperature integral. This method is based on eqs. (5) and (6):

$$\ln\beta = \ln\left(\frac{AE_a}{R}\right) - \ln g(\alpha) - 5.331 - 1.052\left(\frac{E_a}{RT}\right) \tag{5}$$

$$g(\alpha) = \int_0^\alpha \frac{d\alpha}{f(\alpha)} \tag{6}$$

where $g(\alpha)$ is the integral conversion function. This method was used in our computations of $E_a$ at different values of conversion. Thus, for a constant α, the plot of ln β versus $1/T$ (where $T$ is the temperature) obtained from the DSC thermograms with various β's should have rendered a straight line, where the slope allowed the determination of the apparent $E_a$. The experimentally evaluated values of $E_a$ were used to determine the appropriate kinetic model that best described the conversion function of the process studied.

### Friedman method[26]

The Friedman method was used to determine a kinetic model of the curing process. The method is based on eq. (7):

$$\ln\left(\frac{d\alpha}{dt}\right) = \ln\beta\frac{d\alpha}{dT} = \ln[Af(\alpha)] - \frac{E_a}{RT} \tag{7}$$

In case of the $n$th-order reaction

$$f(\alpha) = (1-\alpha)^n \tag{8}$$

$f(\alpha)$ in eq. (7) is substituted by eq. (8):

$$\ln[Af(\alpha)] = \ln\frac{d\alpha}{dt} + \frac{E_a}{RT} = \ln A + n\ln(1-\alpha) \tag{9}$$

The value of $\ln[Af(\alpha)]$ can be obtained from the known values of $\ln[d\alpha/dt]$ and $E_a/RT$. Therefore, the plot of $\ln[Af(\alpha)]$ and $\ln(1-\alpha)$ yields a straight line where the slope corresponds to the reaction order ($n$). The intercept is the natural logarithm of the frequency factor if the reaction mechanism is of $n$th-order kinetics. Otherwise, for an autocatalytic process, the Friedman plot would reveal a maximum of $\ln(1-\alpha)$ approximately around −0.51 to −0.22,

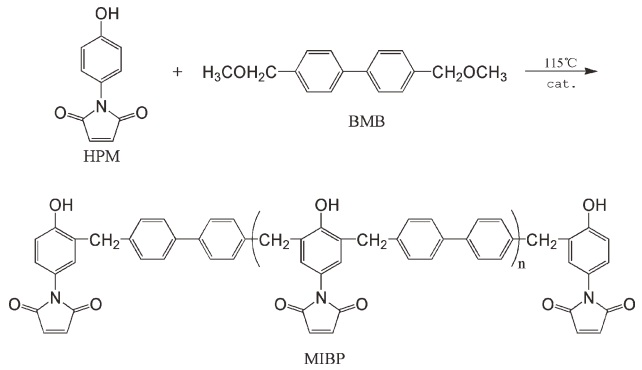


**Scheme 1** Synthetic route to MIBP.

which is equivalent to an α of about 0.2–0.4. This is due to the autocatalytic nature that shows the maximum reaction rate to be at 20–40% conversion.

## RESULTS AND DISCUSSION

### Synthesis and characterization

The preparation of the MIBP was performed through the condensation polymerization of BMB and HPM with *p*-TSA as a catalyst. Temperature control was critical in the reaction because the thermal self-polymerization of the C=C of the maleimide in HPM would occur if the temperature was higher than 120°C.[27]

The synthetic route is given in Scheme 1. GPC measurement of the product and two raw materials was carried out, and the results are shown in Figure 1. The results show the absence of free BMB or HPM in the purified product. We could also see that the resulting product (MIBP) was a mixture of oligomeric compounds. The GPC spectra showed that the

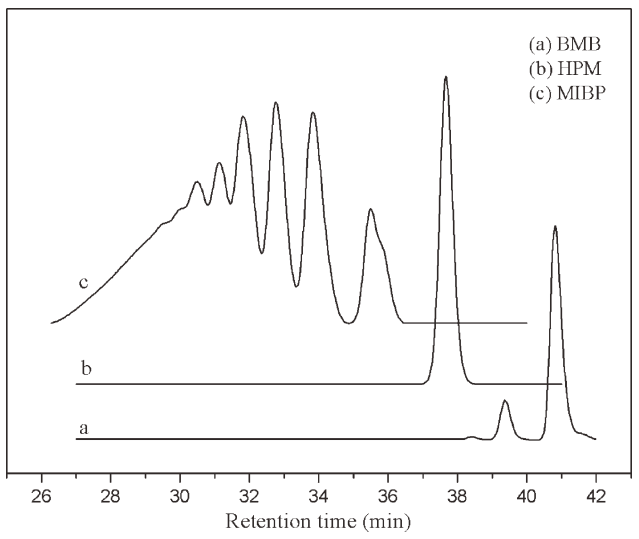


**Figure 1** GPC curves of MIBP and the two monomers (HPM and BMB).

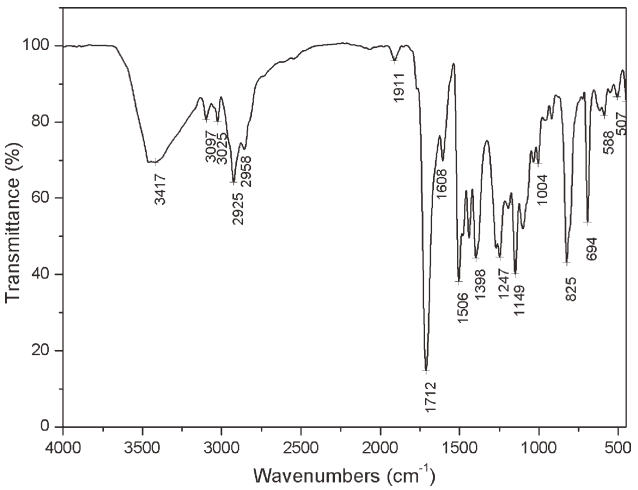


**Figure 2** FTIR spectrum of MIBP.

number-average molecular weight of MIBP was 1100 g/mol and the weight-average molecular weight was 1548 g/mol, with a polydispersity index (PDI) value of 1.41. These results indicate that the majority of the polymers possessed two or three repeat units ($n = 2$ or 3) with a relative low polydispersity.

The structure of the synthesized MIBP was confirmed by FTIR spectroscopy, as shown in Figure 2. The absorption peaks derived from the cyclic maleimide group were observed at 1712 $cm^{-1}$ (C=O symmetric stretching), 1149 $cm^{-1}$ (C—N—C stretching), 1398 $cm^{-1}$ (O=C—N stretching), 694 $cm^{-1}$ (C=C—H bending), and 1608 $cm^{-1}$ (stretching of C=C).[20,27] Additionally, the absorption in the range 3300–3500 $cm^{-1}$ was assigned to the phenolic hydroxyl groups in MIBP.

MIBP was solvable in most of the industrial-use solvents, such as ethylene acetate, acetone, dimethyl sulfoxide, methyl ethyl ketone, *N,N*-dimethylacetamide, tetrahydrofuran, chloroform, and *N,N*-dimethylformamide. The good organosolubility of MIBP suggested its good processability, associated with the current industrial processes.

### Curing reactions of MIBP with CNE

Nonisothermal DSC scans at five different β's recorded at 2.5, 5, 10, 15, and 20°C/min were performed, and the responses are shown in Figure 3. It could be observed that the exothermic peak shifted to a higher temperature with higher β. It was noteworthy that the exotherm showed two overlapping exothermic peaks, although the first exothermic peak was not very distinct. This may imply that there were at least two exothermic reactions occurring during the temperature range 120–250°C. The first exothermic peak, at the lower temperature, was assigned to the polymerization of maleimide C=C bonds (reaction 1), and the second one, occurring at

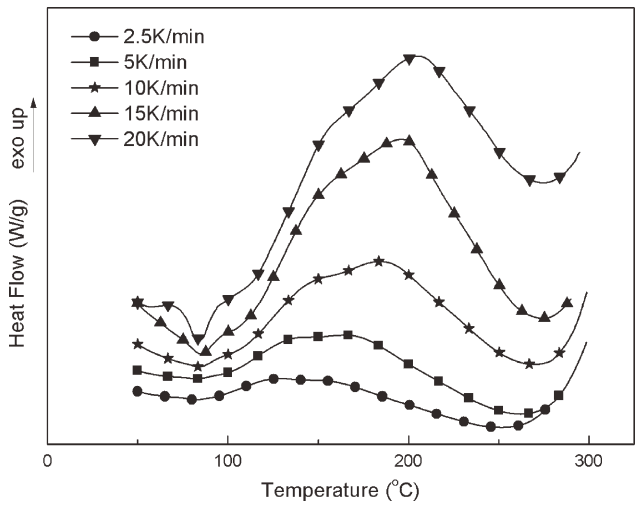


**Figure 3** DSC scans of the CNE/MIBP mixture at different β's.

the higher temperature, was caused by the reactions between phenolic hydroxyls and epoxy groups (reaction 2).

To verify the two curing reactions of the CNE/MIBP mixture, the FTIR spectra of the CNE/MIBP mixture after each curing period were recorded by an FTIR spectrometer, as shown in Figure 4. The spectra showed that there were no significant changes for the sample cured at 130°C for 1 h compared with the uncured mixture at room temperature, except that the adsorption peak at 1149 $cm^{-1}$ (C—N—C of maleimide), which represented the existence of the maleimide ring, became slightly smaller. This indicated that the self-addition of maleimide took place at this curing stage. After the sample was cured at 180°C for 2 h, however, a decrease in the intensity of the absorption peak of C=C at 694 $cm^{-1}$ was observed. Meanwhile, the intensity of the absorption peak at 1149 $cm^{-1}$ decreased because of the translation of maleimide structure to succinimid.[28] The results reveal the decrease of C=C in the maleimide alone with the self-addition reactions of maleimide during this curing stage. After curing at 220°C for 2 h, the reaction of the phenolic hydroxyls and epoxy groups was observed with a decrease in the intensity of the absorption band at 3500 $cm^{-1}$ (phenolic hydroxyl) and 913 $cm^{-1}$ (epoxy group). On the basis of the previous discussion, the curing reactions of CNE with MIBP compounds could be considered to involve two reactions, including maleimide self-addition at above 120°C and the reaction of epoxy groups/hydroxyl group at higher temperatures. These two kinds of reactions during the curing process agreed with the two exothermic peaks exhibited in the DSC curves.

The kinetic analysis of the DSC curves for the CNE/MIBP mixture was carried out by separation of the two overlapping exothermic peaks with the Gaussian distribution function from the PeakFit version 4.12 program (Systat corp. Chicago) and analysis of the distinct characteristic of each exothermic peak. As an exemplification, the DSC thermogram for the curing reaction of the CNE/MIBP mixture at a β of 20°C/min (solid line) and the calculated data from Peakfit version 4.12 (dash line) with two resolved peaks of reaction 1 and reaction 2 (peak 1-filled circles and peak 2-unfilled circles) are illustrated in Figure 5.

## Kinetic model

To study the kinetic models of both reactions occurred in the CNE/MIBP mixture, a complete assessment of the apparent $E_a$ of the CNE/MIBP system throughout the entire conversion range was acquired with the isoconversional method, that is, the Flynn–Wall–Ozawa method. According to eq. (5), for a constant α, if the plot of ln β versus $(1/T)$ fell into a straight line, the slope should have then corresponded to $E_a/R$ at the particular conversion. For instance, Figure 6 is the Flynn–Wall–Ozawa plot of two exothermic peaks of the CNE/MIBP system for $\alpha = 0.1$–$0.9$. A good linear relationship was observed from the Flynn–Wall–Ozawa plots. The values of $E_a$ of each reaction obtained in this manner at different degrees of curing are shown in Figure 7. From the plot, the dependence of the apparent $E_a$'s of both reactions as a function of the curing degree was observed. For each reaction, it could be seen that the $E_a$ values tended to decrease slightly with the degree of conversion; this may have been caused by mass-transfer processes, such as viscous relaxation and vitrification, at the near end of conversion. Therefore, the means of the $E_a$ value determined at α

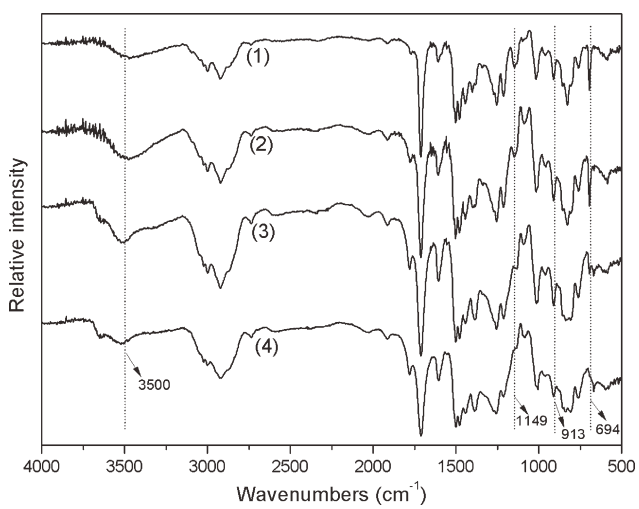


**Figure 4** FTIR spectra of the CNE/MIBP mixture after each curing period: (1) no curing, (2) 130°C (1 h), (3) 180°C (2 h), and (4) 220°C (2 h).

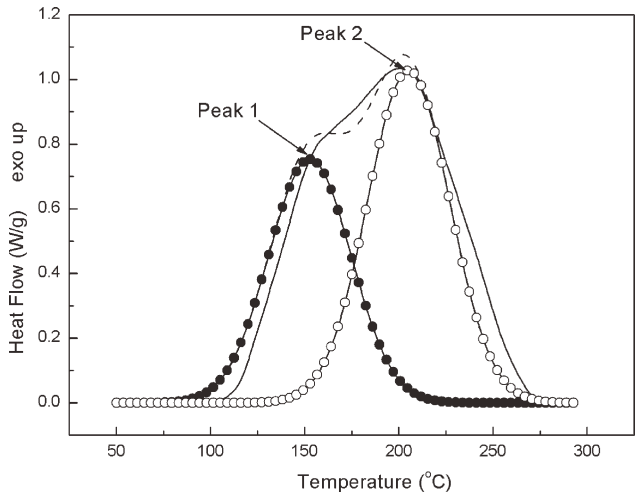


**Figure 5** DSC thermograms of CNE/MIBP at 20°C/min: (—) the DSC thermogram (solid line) and (- - -) the calculated DSC thermogram (dash line) for (●) reaction 1 and (○) reaction 2.

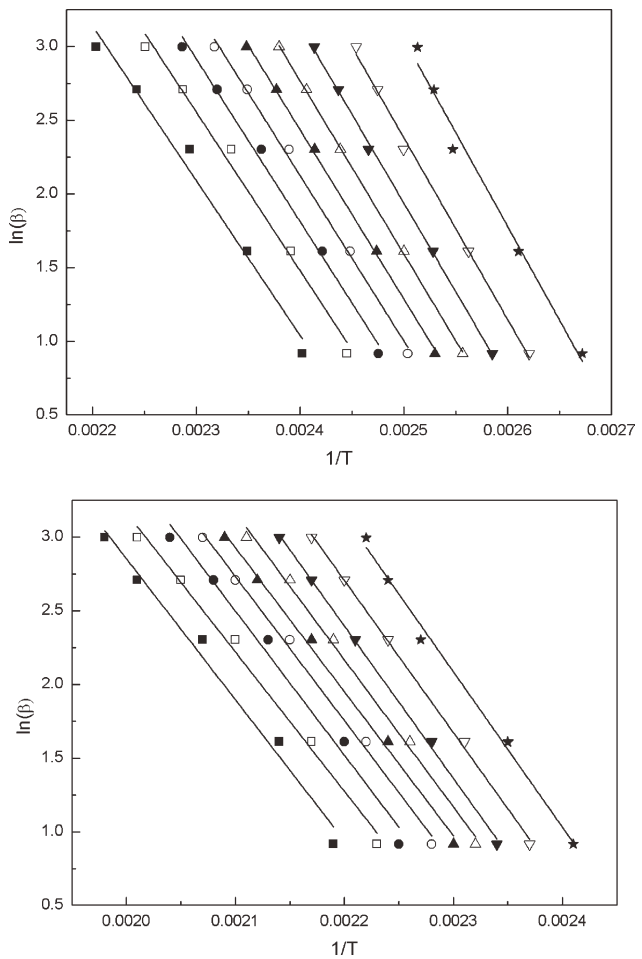


**Figure 6** Flynn–Wall–Ozawa plots of the CNE/MIBP mixture at various degrees of curing (reaction 1, top; reaction 2, bottom): α = (★) 0.1, (▽) 0.2, (▼) 0.3, (△) 0.4, (▲) 0.5, (○) 0.6, (●) 0.7, (□) 0.8, and (■) 0.9.

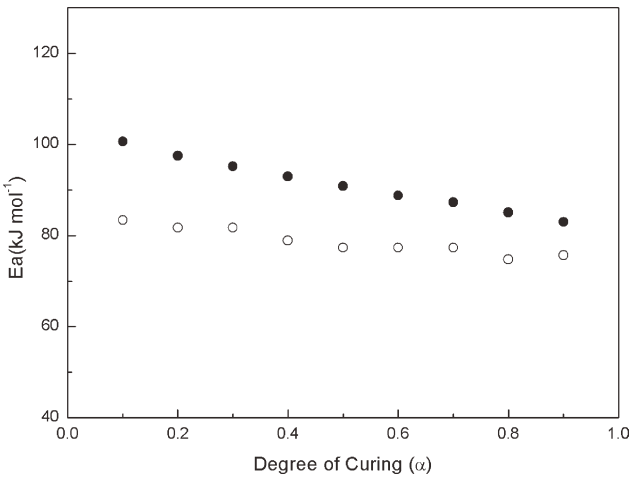


**Figure 7** Values of the apparent $E_a$ obtained from Flynn–Wall–Ozawa plots at different degrees of curing: (●) reaction 1 and (○) reaction 2.

in the range 0.1–0.9, which could be used as apparent $E_a$, were found to be 91.2 kJ/mol for reaction 1 and 78.7 kJ/mol for reaction 2.

We also observed that the average $E_a$ value of reaction 2 was slightly higher but not significantly higher than that of the CNE/PN system (72.2 kJ/mol).[29] This may have further implied that the nature of reaction 2 of the CNE/MIBP system curing was related to the reaction between the epoxy group of CNE and the hydroxyl group of MIBP. The relatively lower reactivity of hydroxyls of MIBP toward epoxy groups was probably due to the steric hindrance of bulky biphenyls and stable imide structures, which reduced its diffusion rate during the curing process. Similar discussions and conclusions are also found in the fluorene and naphthalene-containing epoxy resins.[30,31] However, the reactivity of

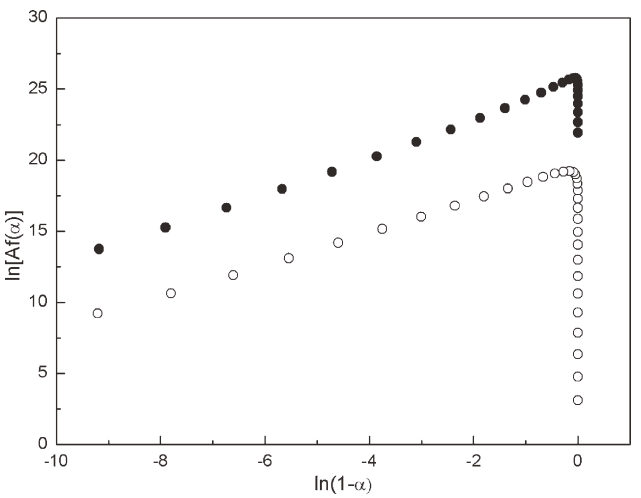


**Figure 8** Plots of ln[$Af(\alpha)$] versus ln(1 − α) of CNE/MIBP mixture with a β of 20°C/min: (●) reaction 1 and (○) reaction 2.

**TABLE I**
**Evaluated Kinetic Parameters for the Curing of the CNE/MIBP System (Reaction 1)**

| β (°C/min) | $E_a$ (kJ/mol) | ln $A$ ($s^{-1}$) | Mean | $n$ | Mean |
|---|---|---|---|---|---|
| 2.5 | 91.2 | 25.94 | 25.92 | 1.35 | 1.42 |
| 5 | | 25.93 | | 1.30 | |
| 10 | | 25.91 | | 1.46 | |
| 15 | | 25.89 | | 1.58 | |
| 20 | | 25.91 | | 1.38 | |

MIBP toward CNE resin was not significantly affected by the introduction of the maleimide and biphenyl moieties.

To find the kinetic model, the Friedman method employed in this work requires the previously known $E_a$ value. In our case, the average $E_a$ values obtained from Flynn–Wall–Ozawa method were used for the determination of each $n$ of the CNE/MIBP system. In general, the mechanisms of thermoset curing are classified into two major kinetic reactions, $n$th-order and an autocatalytic reactions.[32] For the $n$th-order reaction, the average $E_a$ from the Flynn–Wall–Ozawa method was taken as a constant, and eq. (9) may be written as follows:

$$\ln[Af(\alpha)] = \ln A + n\ln(1-\alpha) \tag{10}$$

Friedman suggested that the relationship between $\ln[Af(\alpha)]$ and $\ln(1-\alpha)$ should yield a straight line, in which the slope corresponds to $n$. Otherwise, for autocatalytic process, the Friedman plot would show a maximum of $\ln(1-\alpha)$ approximately around $-0.51$ to $-0.22$, which is equivalent to $\alpha$ of about 0.2–0.4.

Figure 8 depicts Friedman plots as an exemplification of the reactions 1 and 2 of the CNE/MIBP system at a β of 20°C/min. For both reactions, because $\ln[Af(\alpha)]$ and $\ln(1-\alpha)$ are perfectly linearly related in the range of the degree of conversion mentioned previously, this suggested that both curing reactions were $n$th order in nature.

Therefore, for the $n$th-order model, the kinetic parameters $n$ and $A$ could be obtained by the slope of the linear dependence $\ln[Af(\alpha)]$ versus $\ln(1-\alpha)$, according to the eq. (10). The results of the kinetic

**TABLE II**
**Evaluated Kinetic Parameters for the Curing of the CNE/MIBP System (Reaction 2)**

| β (°C/min) | $E_a$ (kJ/mol) | ln $A$ ($s^{-1}$) | Mean | $n$ | Mean |
|---|---|---|---|---|---|
| 2.5 | 78.7 | 19.68 | 19.66 | 1.12 | 1.11 |
| 5 | | 19.83 | | 1.12 | |
| 10 | | 19.86 | | 1.11 | |
| 15 | | 19.61 | | 1.12 | |
| 20 | | 19.30 | | 1.10 | |

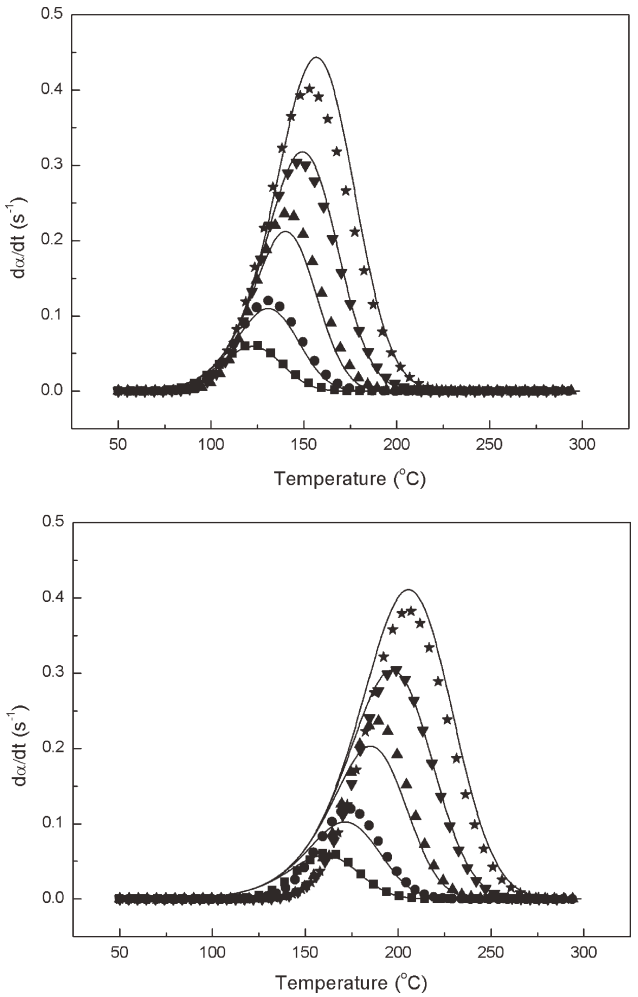


**Figure 9** Experimental (symbols) and calculated (solid lines) DSC peaks corresponding to the curing process of the CNE/MIBP mixture (reaction 1, top; reaction 2, bottom): (■) 2.5, (●) 5, (▲) 10, (▼) 15, (★) 20°C/min.

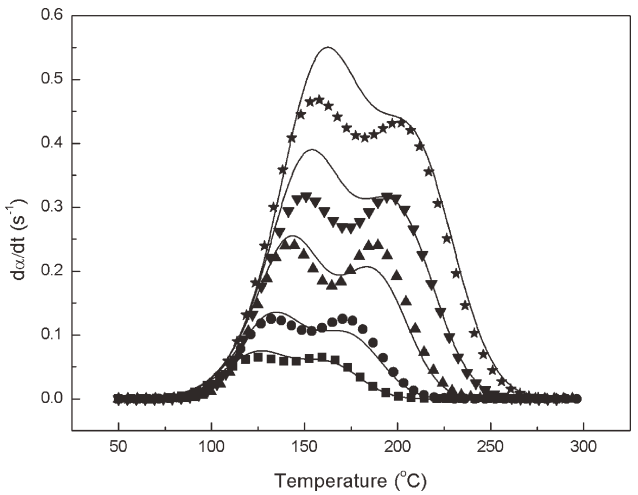


**Figure 10** Experimental (symbols) and calculated (solid lines) DSC peaks corresponding to the curing process of the CNE/MIBP mixture of the total curing reaction: (■) 2.5, (●) 5, (▲) 10, (▼) 15, and (★) 20°C/min.

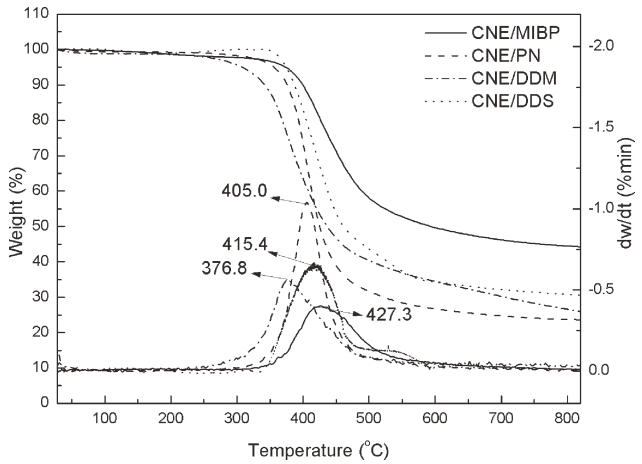


**Figure 11** TGA thermograms of cured epoxy resins in a nitrogen atmosphere. *dw/dt*, derivative weight.

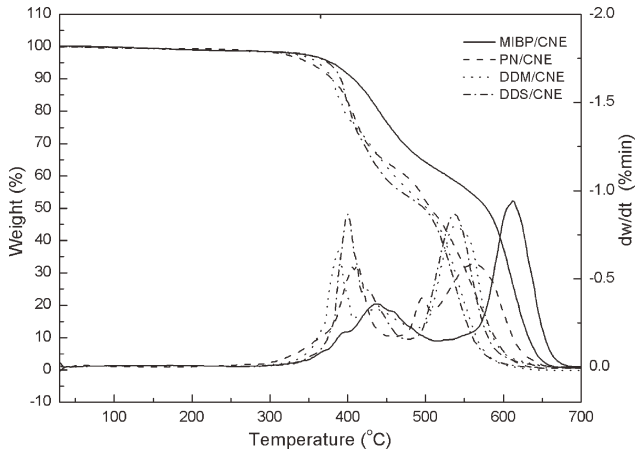


**Figure 12** TGA thermograms of the cured epoxy resins in an air atmosphere.

parameters for all β's of reaction 1 and reaction 2 are listed in Tables I and II, respectively.

The experimental curves and predicted curves based on the determined kinetic parameters of the curing reaction for peak 1 and peak 2 at different β's are shown in Figure 9. It is clearly shown that the calculated data from the model are in good agreement with the experimental results. Furthermore, the curing rates of reaction 1 ($d\alpha_1/dt$) and reaction 2 ($d\alpha_2/dt$) were a function of total α, which was equal to the sum of $\alpha_1$ and $\alpha_2$. The correlations of those conversions are shown in eq. (11).

$$\frac{d\alpha}{dt} = \frac{d\alpha_1}{dt} + \frac{d\alpha_2}{dt} \tag{11}$$

The plots of the total α with respect to temperature could be obtained from eq. (11), and the results are plotted in Figure 10. From this figure, the calculated DSC curve fit relatively well with the experimental data with the obtained models.

### Thermal properties of the cured epoxy resins

The thermal stability of the cured CNE/MIBP system was assessed by TGA under both nitrogen and air atmospheres, and the results are shown in Figures 11 and 12. The thermal stabilities of these blends were compared by consideration of the temperatures for 5% ($T_{5\%}$) and 10% ($T_{10\%}$) weight loss, the maximum weight loss temperature ($T_{max}$), and the char yields at 600 and 800°C. These data are presented in Table III.

According to Figures 11 and 12 and Table III, $T_{5\%}$ and $T_{max}$ values of the CNE/MIBP polymer both in $N_2$ and in air were much higher than those of the controlled ones. These results indicate that the introduction of a stable imide structure and a bulky biphenyl skeleton into the epoxy resin improved the inherent thermal stability of the thermosets dramatically. Significantly, the incorporation of maleimide groups, which underwent a self-addition reaction during the thermal curing process, contributed to the degree of crosslinking. The relatively high char yield of the CNE/MIBP polymer could have been due to the higher crosslink density of the curing system. This may suggest that the condensed aromatic rings (biphenyl) and higher crosslink density facilitated the formation of char.[33]

To better understand the TGA results, the residue char under a nitrogen atmosphere (800°C) was characterized with FTIR spectroscopy and XRD, as shown

**TABLE III**
**Thermal Properties of the Cured Epoxy Resin**

| | | Weight-loss temperature (°C) | | | | $T_{max}$ (°C) | | | | Char yield (%) | | | |
|---|---|---|---|---|---|---|---|---|---|---|---|---|---|
| | | $T_{5\%}$ | | $T_{10\%}$ | | Step 1 | | Step 2 | | 600°C | | 800°C | |
| Sample | $T_g$ (°C)[a] | Air | $N_2$ | Air | $N_2$ | Air | $N_2$ | Air | $N_2$ | Air | $N_2$ | Air | $N_2$ |
| CNE/MIBP | 155 | 379 | 372 | 408 | 400 | 437 | 427 | 612 | — | 38.2 | 49.8 | 0 | 44.5 |
| CNE/PN | 143 | 350 | 355 | 380 | 376 | 412 | 405 | 564 | — | 5.8 | 26.7 | 0 | 23.7 |
| CNE/DDM | 110 | 361 | 306 | 379 | 342 | 387 | 376 | 538 | — | 1.7 | 34.4 | 0 | 26.6 |
| CNE/DDS | 133 | 374 | 374 | 390 | 387 | 400 | 415 | 537 | — | 2.0 | 34.5 | 0 | 30.8 |

An em dash indicates that step 2 for the maximum weight loss was not found.
[a] The $T_g$ values for CNE/PN, CNE/DDM, and CNE/DDS were obtained from the literature.[16,21,35]

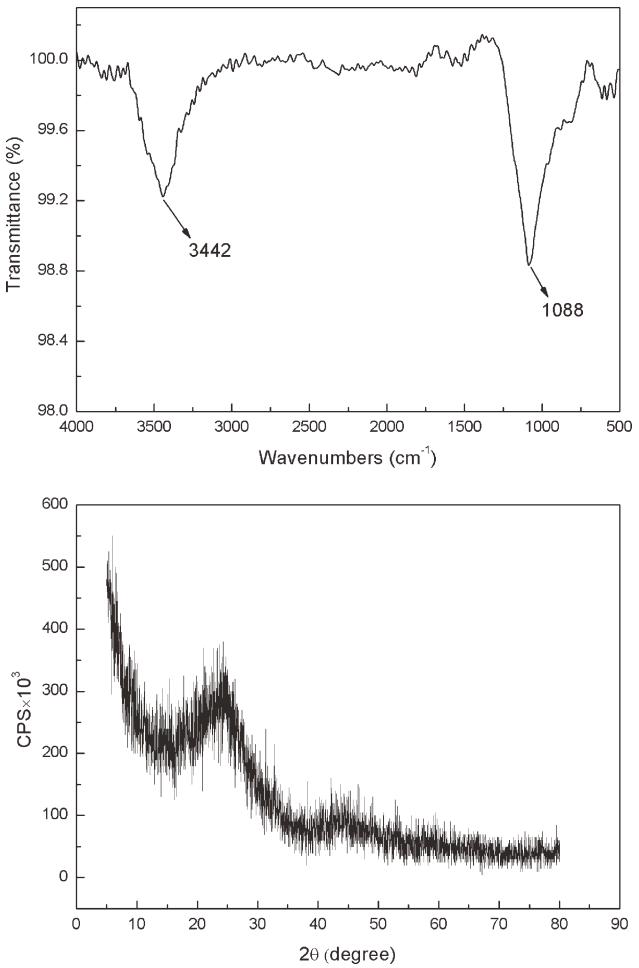


**Figure 13** FTIR spectrum (top) and XRD pattern (bottom) of the residue char of TGA under an $N_2$ atmosphere. CPS, counts per second.

in Figure 13. The FTIR spectrum of the pyrolyzed CNE/MIBP polymer showed a weak broad absorption at 950–1150 $cm^{-1}$. This may have been due to the residual C—O linkages present in the system. It might not have been possible to completely eliminate the oxygen atom under the limited pyrolysis temperature. C—OH absorptions were observed at 3300–3600 $cm^{-1}$. The FTIR spectra resembled that of commercial charcoal. From the XRD pattern, we could see that the char turned out to be amorphous in nature, which agreed with the works reported by Nair et al.[34]

The glass-transition temperature ($T_g$) of the CNE/MIBP polymer was determined by DSC. The result is shown in Figure 14 and compared in Table III. It was noteworthy that the $T_g$ of CNE/MIBP (155°C) was higher than those of the controls. This result may confirm that $T_g$ of the cured polymers could be elevated drastically by the introduction of the rigid biphenyl group into the epoxy resins, which could have restrained the thermal movements.

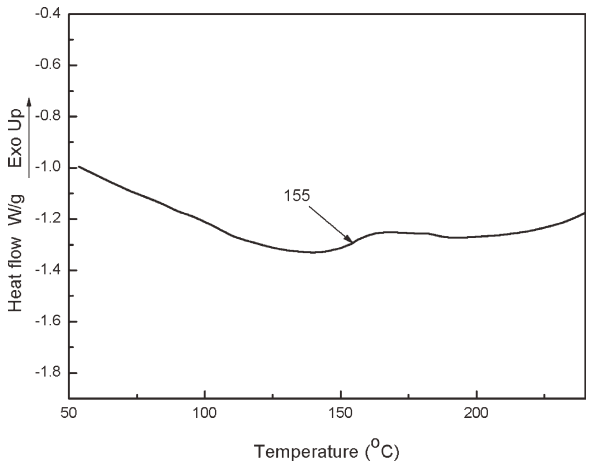


**Figure 14** DSC scans of the CNE/MIBP polymer for determining $T_g$.

## CONCLUSIONS

MIBP was synthesized and used as a macromolecular curing agent for CNE resin. The curing characteristics of the CNE/MIBP system were studied by DSC and showed a two-stage curing process. FTIR spectroscopy was used to verify the reactions of each curing process, and the results indicate that the first peak in the DSC curve was due to the self-addition of maleimide and the second one was responsible for the reaction of epoxy groups/hydroxyl groups.

The cure kinetics of each curing reaction of the CNE/MIBP blend were studied by isoconversional methods, the Flynn–Wall–Ozawa and Friedman methods, and the results show that each of reactions exhibited *n*th-order curing kinetics with different *n* values. Evidently, the kinetic models for the curing reactions of the both reactions were in good agreement with the nonisothermal DSC results.

Compared with conventional curing agents (PN, DDM, DDS), the cured epoxy with MIBP exhibited a higher $T_g$ ($T_g$ = 155°C), good thermal stability ($T_{10\%}$ under nitrogen and in air ≈ 400 and 408°C, respectively), and high char yield ($T$ = 800°C, char residue = 44.5% under nitrogen). The introduction of stable maleimide and rigid biphenyl moieties into the epoxy resin was considered to be responsible for the combination of these good thermal properties.

## References

1. Wu, C. S.; Liu, Y. L.; Hsu, K. Y. Polymer 2003, 44, 565.
2. Zuo, C.; Han, J.; Si, Z.; Xue, G. J Appl Polym Sci 2009, 114, 3889.
3. Mustata, F.; Bicu, I. Polymer 2010, 115, 1787.
4. Zhang, X. H.; Xia, X. N.; Xu, W. J.; Xiong, Y. Q. Eur Polym J 2007, 43, 2149.
5. Kaji, M.; Nakahara, K.; Ogami, K.; Endo, T. J Polym Sci Part A: Polym Chem 1999, 37, 3687.
6. Guo, Q.; Huang, Y.; Zhang, Y. Y.; Zhu, L. R.; Zhang, B. L. J Therm Anal Calorim 2010, 102, 915.
7. Wang, C. S.; Lee, M. C. Polym Bull 1998, 40, 623.

8. Ren, H.; Sun, J. Z.; Wu, B. J.; Zhou, Q. Y. Polymer 2006, 47, 8309.
9. Liu, W. C.; Varley, R. J.; Simon, G. P. Polymer 2006, 47, 2091.
10. Gouri, C.; Reghunadhan Nair, C. P.; Ramaswamy, R. J Appl Polym Sci 1999, 73, 695.
11. Rao, B.; Sireesha, R.; Pasala, A. Polym Int 2005, 54, 1103.
12. Wang, M. W.; Wu, H. Y.; Lin, M. S. J Polym Res 2008, 15, 1.
13. Shu, W. J.; Yang, B. Y.; Chin, W. K.; Perng, L. H. J Appl Polym Sci 2002, 84, 2080.
14. Liu, X.; Xin, W.; Zhang, J. Bioresour Technol 2010, 101, 2520.
15. Sharma, P.; Choudhary, V.; Narula, A. K. J Appl Polym Sci 2006, 101, 3503.
16. Wu, W. L.; Hsu, K. C.; Cheng, W. H. J Appl Polym Sci 2008, 108, 2052.
17. Bindu, R. L.; Nair, C. P. R.; Ninan, K. N. J Polym Sci Part A: Polym Chem 2000, 38, 641.
18. Chin, W. K.; Hwu, J. J.; Shau, M. D. Polymer 1998, 39, 4923.
19. Li, H. T.; Chuang, H. R.; Wang, M. W.; Lin, M. S. Polym Int 2005, 54, 1416.
20. Liu, Y. L.; Chen, Y. J.; Wei, W. L. Polymer 2003, 44, 6465.
21. Xia, X. N.; Xiong, Y. Q.; Zhang, X. H.; Xu, W. J. J Appl Polym Sci 2006, 102, 3843
22. Sbirrazzuoli, N.; Vyazovkin, S. Thermochim Acta 2002, 388, 289.
23. He, Y. Thermochim Acta 2001, 367, 101.
24. Kissinger, H. E. Anal Chem 1957, 29, 1702.
25. Ozawa, T. Bull Chem Soc Jpn 1965, 38, 1881.
26. Friedman, H. L. J Polym Sci Part C: Polym Symp 1965, 6, 183.
27. Liu, Y. L.; Yu, J. M.; Chou, C. I. J Polym Sci Part A: Polym Chem 2004, 42, 5954
28. Mison, P.; Sillion, B. Adv Polym Sci 1998, 40, 137.
29. Xia, X. N. Study on Synthesis and Properties of Phosphorous/nitrogen- containing flame retardant Epoxy Resin [D] 2006.
30. Lin, C. H.; Yang, K. Z.; Leu, T. S.; Lin, C. H.; Sie, J. W. J Polym Sci Part A: Polym Chem 2006, 44, 3487.
31. Liu, W.; Qiu, Q.; Wang, J.; Huo, Z.; Sun, H. Polymer 2008, 49, 4399.
32. Prime, R. B. Thermosets. In Thermal Characterization of Polymeric Materials; Turi, E. A., Ed.; Academic: San Diego, 1997; Chapter 6.
33. Liu, W.; Qiu, Q.; Wang, J.; Huo, Z.; Sun, H. Polymer 2008, 49, 4399.
34. Bindu, R. L.; Nair, C. P.; Ninan, K. N. J Appl Polym Sci 2001, 80, 1664.
35. Rwei, S. P.; Cheng, C. Y.; Liou, G. S.; Cheng, K. C. Polym Eng Sci 2005, 45, 478.